Chapter 6

NMR Spectroscopy Approach to Study the Structure, Orientation, and Mechanism of the Multidrug Exporter EmrE

Maureen Leninger and Nathaniel J. Traaseth

Abstract

Multidrug exporters are a class of membrane proteins that remove antibiotics from the cytoplasm of bacteria and in the process confer multidrug resistance to the organism. This chapter outlines the sample preparation and optimization of oriented solid-state NMR experiments applied to the study of structure and dynamics for the model transporter EmrE from the small multidrug resistance (SMR) family.

Key words Solid-state NMR, PISEMA, NMR pedagogy, Membrane proteins, Multidrug resistance, Bicelles

1 Introduction

Drug efflux by membrane transport proteins is a primary mechanism bacteria use to confer resistance to antiseptics and antibiotics [1–3]. These multidrug transporters bind and efflux lethal compounds from the cytoplasm and in the process reduce the toxicity to the organism. Several transporter structures have been determined using X-ray crystallography, which have provided detailed insight into the transport process (reviewed in [4]). A complementary method for resolving the mechanism of ion-coupled transport is through the use of nuclear magnetic resonance (NMR) spectroscopy. One advantage of this approach is to study efflux pumps under conditions that mimic the native membrane environment. This chapter describes how oriented solid-state NMR (O-SSNMR) spectroscopy is used to directly interrogate the structure of the drug transporter EmrE from the small multidrug resistance (SMR) family. The anisotropic observables offered from these experiments (e.g., anisotropic chemical shifts and dipolar couplings) are used as restraints in structure determination and are excellent reporters of the tilt and rotation angles for transmembrane proteins within the lipid bilayer (Fig. 1) [5–11].

Akihito Yamaguchi and Kunihiko Nishino (eds.), *Bacterial Multidrug Exporters: Methods and Protocols*, Methods in Molecular Biology, vol. 1700, https://doi.org/10.1007/978-1-4939-7454-2_6,

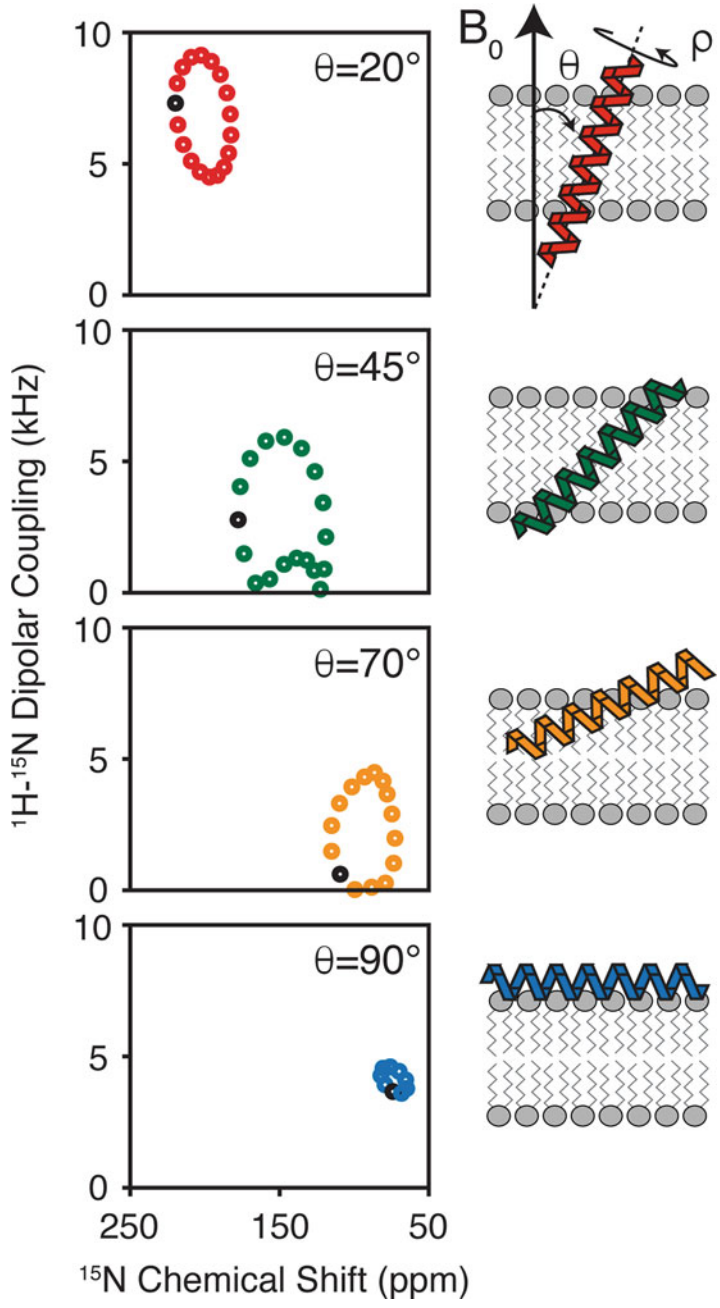

Fig. 1 Calculated separated local field spectra of ^{1}H-^{15}N dipolar coupling vs. ^{15}N anisotropic chemical shift for an ideal helix. The periodic spectral patterns are sensitive to the tilt and rotation angles of the secondary structures with respect to the magnetic field. These patterns have been termed PISA wheels [7, 9]

The prerequisite for using O-SSNMR to characterize membrane protein structures is to align the samples within the magnetic field. This is most commonly accomplished using mechanical alignment of lipid bilayers absorbed onto glass plates [12, 13] or

magnetic alignment with lipid bicelles [14]. The former approach has been successfully applied for multiple membrane proteins including M2 from the influenza A virus [15] and the muscle regulatory protein phospholamban [16]. For EmrE, we utilize lipid bicelle technology due to the excellent control of sample hydration and improved alignment with respect to the magnetic field [17]. Specifically, our experiments use a bicelle composition of DMPC (14:0) and DHPC (6:0) at a 3.2/1 molar ratio, which readily forms aligned liquid crystals at 37 °C [18–21]. Replacing the DMPC component with a shorter (12:0) or longer (16:0) chain phosphatidylcholine lipid can be used to lower or raise the alignment temperature, respectively [22–24]. In addition, the usage of POPC in combination with DMPC can also reduce the alignment temperature to 25 °C [17]. One of the most important requirements of bicelle selection is to ensure protein stability in the chosen lipid composition [20]. Finally, since the quality of protein alignment can be protein dependent, the lipid to protein ratio should be optimized in an empirical fashion to ensure bicelle alignment in the magnetic field. For EmrE, we find that a lipid to protein ratio of 150:1 (mol:mol) is effective to achieve good signal to noise without compromising the overall alignment with respect to the magnetic field.

Below we discuss the procedure of bicelle sample preparation containing EmrE and the setup of the polarization inversion spin exchange at the magic angle (PISEMA) experiment [25, 26], which is a sensitive way to probe secondary structural information with respect to the membrane. Using this experiment and others, we have resolved the asymmetric monomer subunits within the EmrE homodimer and quantified conformational exchange dynamics of the transporter that are required for drug efflux [27, 28].

2 Materials

2.1 Sample Preparation

1. Isotopically ^{15}N-enriched protein: modify the expression conditions for your favorite protein with the addition of $^{15}NH_4Cl$ to M9 minimal media to obtain uniformly ^{15}N-enriched proteins or the addition of one or several ^{15}N-labeled amino acids for selectively enriched proteins.
2. *n*-Dodecyl-β-D-maltoside (DDM).
3. *n*-Octyl-β-D-glucoside (OG).
4. Bio-Beads™ SM-2 resin, Bio-Rad Laboratories.
5. Ultracentrifuge: instrument should reach centrifugal forces of at least 150,000 × *g*.
6. 1,2-Dimyristoyl-*sn*-glycero-3-phosphocholine (DMPC), Avanti Polar Lipids, Inc.

7. 1,2-Dihexanoyl-*sn*-glycero-3-phosphocholine (DHPC), Avanti Polar Lipids, Inc.
8. Ytterbium(III) chloride ($YbCl_3$).

2.2 NMR Instrumentation and Data Analysis

1. Bicelle sample holder assembly (design by Peter Gor'kov at NHMFL, Tallahassee, FL):
   (a) 5 mm open-ended glass tube, New Era Enterprises, part No. NE-RG5-P-17-OE-BOE.
   (b) B5 plugs with and without fill hole, Revolution NMR, part No. MP4763-001 and MP4764-001.
2. Solid-state NMR spectrometer: our experiments were carried out using an Agilent DD2 spectrometer operating at a ^{1}H Larmor frequency of 600 MHz.
3. Solid-state NMR probes capable of ^{31}P and ^{15}N detection. Our experiments use the following:
   (a) BioStatic H-X probe with 5 mm bicelle coil tuned to ^{31}P on the X-channel (Agilent).
   (b) *Low-E* ^{1}H-^{15} N probe with 5 mm bicelle coil for ^{15}N detection (probe design by Peter Gor'kov) [29]. This probe technology is commercially available from Revolution NMR, LLC (www.revolutionnmr.com).
4. NMR data processing software: NMRPipe [30] and Sparky v3.113 (T.D. Goddard and D. G. Kneller, SPARKY 3, University of California, San Francisco).

3 Methods

3.1 Sample Preparation

EmrE is expressed from a pMAL™ vector (New England Biolabs) where maltose binding protein (MBP) is positioned on the N-terminal side of the EmrE gene. The expression is performed in *E. coli* BL21(DE3) cells in minimal media using selectively labeled ^{15}N amino acids or $^{15}NH_4Cl$ to uniformly enrich the protein. EmrE is purified with an amylose affinity column, cleaved with TEV protease to remove MBP, and passed over a size exclusion column as previously described [27, 28]. Purified EmrE in DDM detergent micelles is then reconstituted into DMPC lipid bilayers. Below is the reconstitution procedure:

1. 28 mg DMPC is hydrated with 1 mL of 20 mM sodium phosphate and 20 mM NaCl and subjected to multiple cycles of flash freezing.
2. Bath sonicate the sample for 15 min.
3. Add 5.6 mg OG to the mixture and equilibrate for 10 min.

4. Add 7 mL EmrE at a concentration of 0.5 mg/mL in DDM detergent to the sonicated lipids. Additional DDM may be added to ensure the lipids are solubilized, which will be evident when the mixture becomes clear. Typically, a total of ~30 mg DDM is added including the detergent with EmrE.
5. Incubate the sample for 1 h at room temperature.
6. Add 2.25 g of Bio-Beads to give a final ratio of 75 mg per mg of detergent.
7. Gently stir for 12 h at 4 °C. Note that the removal of detergent by the Bio-Beads will instigate formation of proteoliposomes and lead to a slightly cloudy solution.
8. Remove Bio-Beads from the suspension.
9. Centrifuge proteoliposomes in a Beckman Optima MAX_XP TLA 110 rotor at 100,000 × *g* for 1.5 h.
10. Resuspend the liposome pellets in 100 mM HEPES and 20 mM NaCl (pH 7) buffer and freeze thaw 5–10 times to exchange the buffer.
11. Centrifuge the sample in the TLA 110 rotor for 2.5 h at 150,000 × *g*.
12. Add 25 μL of 425 mM DHPC in water to the proteoliposome pellet. This corresponds to a DMPC:DHPC molar ratio ("*q* value") of ~3.2–3.5 (*see* **Note 1**).
13. Mix thoroughly by a combination of vortexing, flash freezing with liquid nitrogen, and heating to 37 °C. After the mixing is complete, the sample should be fluid on ice and a viscous gel at 37 °C (*see* **Note 2**).
14. Centrifuge the sample in a 1.5 mL microcentrifuge tube for 2 min at 500 × *g* using a benchtop centrifuge and place the supernatant in a new microcentrifuge tube.
15. For unflipped bicelle samples (bicelle normal perpendicular to magnetic field), proceed to **step 16**. For flipped samples (bicelle normal parallel to magnetic field), add 6 μL of 100 mM $YbCl_3$ to give a final concentration of 4.5 mM (*see* **Note 3**).
16. Place the sample in the bicelle sample holder for O-SSNMR experiments.

3.2 Check Bicelle Alignment with ^{31}P NMR

The alignment of the bicelle in the magnetic field is checked by recording a one-pulse ^{31}P experiment optimized for a 90° tilt angle followed by acquisition of the free induction decay under ^{1}H decoupling with SPINAL-64 [31] This experiment is a sensitive way to check the sample since ^{31}P is 100% natural abundant, has a relatively high gyromagnetic ratio, and is present in both DMPC and DHPC headgroups. Representative ^{31}P spectra of flipped, isotropic and unflipped bicelles are shown in Fig. 2a–c, respectively (*see* **Note 4**).

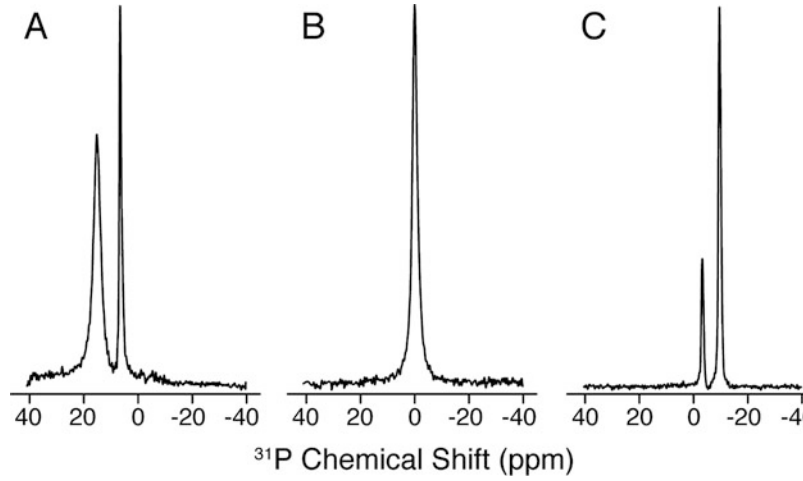

Fig. 2 ^{31}P spectra of lipid bicelle samples. The panels show representative spectra for (**a**) flipped, (**b**) isotropic, and (**c**) unflipped bicelles. The flipped spectra were obtained by the addition of $YbCl_3$

3.3 Optimization of the Polarization Inversion Spin Exchange at the Magic Angle (PISEMA) Experiment

PISEMA is a separated local field experiment to correlate dipolar couplings with anisotropic chemical shifts [25, 26]. The spectral patterns from PISEMA are directly sensitive to the tilt and rotation angles of the protein secondary structures with respect to the magnetic field [7, 9]. PISEMA begins with a cross-polarization (CP) sequence to transfer magnetization from ^{1}H to ^{15}N spins in order to increase the sensitivity of the experiment. Homonuclear dipolar decoupling in the indirect dimension is achieved by frequency-switched or phase-modulated Lee-Goldburg (FSLG or PMLG) [32–35]. Both of these sequences enable evolution of a scaled heteronuclear dipolar coupling in the absence of ^{15}N chemical shift evolution. After evolving the dipolar coupling in the indirect dimension, the PISEMA experiment detects the free precession of the ^{15}N nucleus under high-power ^{1}H decoupling. The most common application of PISEMA is to enrich the protein with ^{15}N labeling and correlate the ^{1}H-^{15}N dipolar coupling with the ^{15}N anisotropic chemical shift (*see* **Note 5**). Advancements in the original PISEMA experiment include developments to reduce the ^{1}H offset dependence of the indirect dimension [36], a sensitivity-enhanced version to improve signal-to-noise [37, 38] and a constant-time experiment to improve the resolution in the dipolar coupling dimension [39].

Prior to data acquisition on the protein sample, it is recommended to first optimize the pulse sequence parameters with two model compounds: (1) an aqueous buffer composed of 100 mM HEPES and 20 mM NaCl (pH 7.0) and (2) a single crystal of ^{15}N-labeled *N*-acetyl-leucine (NAL).

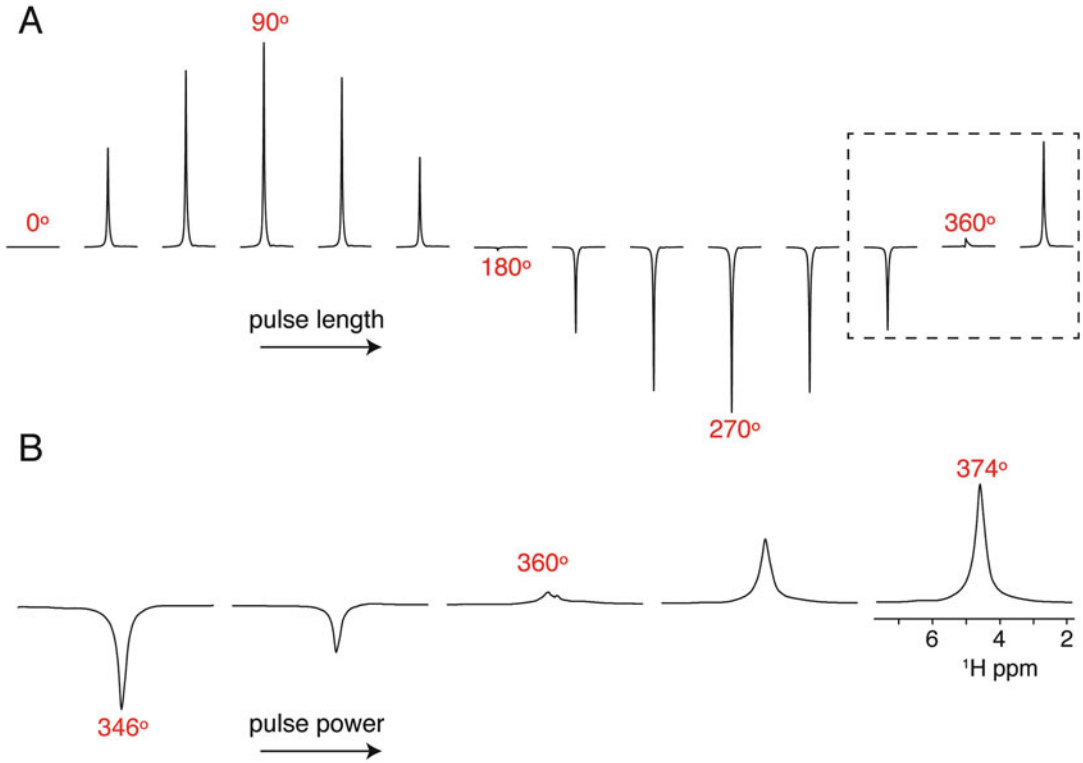

Fig. 3 Optimization of the ^{1}H 90° pulse on the water peak. (**a**) Nutation curve by varying the pulse length at a fixed B_1 amplitude to determine an accurate 360° pulse. (b) Fine tune calibration of the 360° pulse by setting the pulse length to four times the desired 90° pulse and increasing the power level from left to right. The null value corresponds to the 360° pulse

3.3.1 Insert Buffer Sample to Calibrate ^{1}H 90° Pulse Parameters

If the probe requires pulse length calibration for the first time, it is necessary to optimize ^{1}H 90° pulses for a given pulse duration that is within the voltage handling of the probe circuit. This is typically specified by a minimum 90° pulse width that can be applied without damage to the probe. We typically optimize for 5 and 6 μs pulse lengths on the water signal of a sample of 100 mM HEPES and 20 mM NaCl (pH 7.0) by carrying out a full nutation curve where the pulse length is varied at a constant power (Fig. 3a). Next, the pulse power is more finely calibrated to the desired 360° pulse (e.g., 20 or 24 μs, respectively) by adjusting the power level to identify the corresponding null in the spectrum (*see* **Note 6**). An example of the calibration is shown in Fig. 3b.

3.3.2 Insert the N-Acetyl Leucine Single Crystal

1. *Optimize cross-polarization (CP) from ^{1}H to ^{15}N.* There are a few variants of this sequence that provide efficient polarization transfers, including linear and adiabatic ramps as well as CP-MOIST [40, 41] (*see* **Note 7**).

2. *Optimize the 90° pulse for ^{15}N.* The experiment employs a 90° ^{15}N pulse after the CP from ^{1}H to ^{15}N. The signal on ^{15}N is detected under ^{1}H decoupling. The flip back pulse is set to the desired length with the power adjusted in an iterative manner. The null in the spectrum gives the optimal power corresponding to the pulse length.
3. *Calculate the parameters for the indirect dimension of the PISEMA experiment.* For the SEMA portion of PISEMA (i.e., t_1 period), the effective frequency on ^{15}N must match the effective frequency of ^{1}H (i.e., $\omega_{\mathrm{eff},15N} = \omega_{\mathrm{eff},1H}$). The ^{15}N spin-lock during t_1 evolution is on resonance so the effective frequency is equal to applied frequency ($\omega_{1,15N} = \omega_{\mathrm{eff},15N}$) (*see* **Note 8**). Unlike the ^{15}N effective frequency, the ^{1}H effective frequency during FSLG or PMLG is not equal to the applied frequency. For this reason, the frequency offset ($\Delta\omega$) and applied frequency (ω_1) need to be set so that the effective frequency of ^{1}H will match that of ^{15}N ($\omega_{\mathrm{eff},15N} = \omega_{\mathrm{eff},1H}$). A second requirement of PMLG or FSLG is that the effective frequency on ^{1}H is applied at the magic angle in order to average out homonuclear dipolar couplings. Using the trigonometric relationships given in Eqs. 1 and 2 and the desired effective frequencies for ^{15}N and ^{1}H, $\Delta\omega$ and ω_1 can be calculated for ^{1}H (*see* **Note 9**).

$$\tan\theta = \frac{\omega_1}{\Delta\omega} \quad (\theta = 54.7) \tag{1}$$

$$\omega_{\mathrm{eff}}^2 = \omega_1^2 + \Delta\omega^2 \tag{2}$$

4. *Collect the 2D PISEMA experiment.* The PISEMA experiment is collected using the optimized pulse sequence parameters and Fourier transformed to give the resulting two-dimensional spectrum (*see* **Note 10**).
5. *Adjust ^{1}H offset to minimize the zero-frequency.* Since the dipolar coupling frequency measured in the indirect dimension is sensitive to the ^{1}H offset, one can adjust the transmitter frequency for ^{1}H to minimize the zero-frequency signals for desired peaks in the single crystal sample. The optimal ^{1}H offset may be different for the protein sample.

3.3.3 Acquire PISEMA Spectrum on Membrane Protein Sample

1. *Optimize the ^{1}H 90° pulse.* Similar to the pulse calibration on the buffer sample, we optimize for 5 and 6 μs 90° pulse lengths on the water signal in the protein/bicelle sample. As described above and shown in Fig. 3b, the pulse length is set to four times the 90° pulse with the power levels adjusted to find the null.

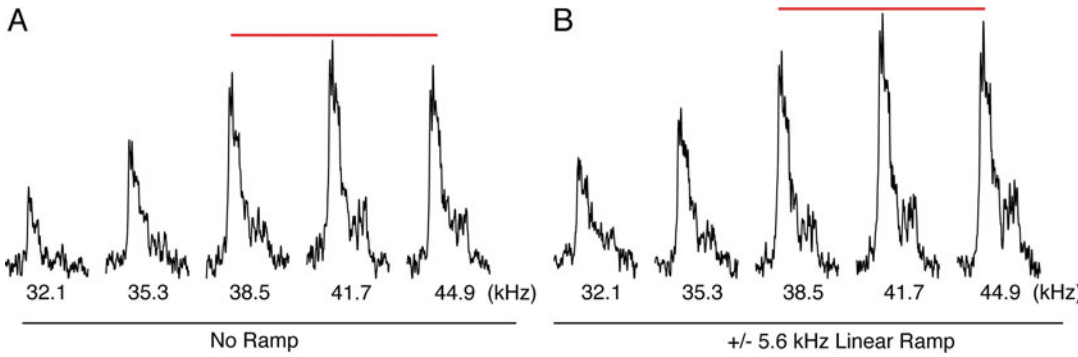

Fig. 4 Optimization of ^{1}H to ^{15}N cross-polarization as demonstrated for EmrE in lipid bicelles. (**a**) The ^{1}H power is arrayed around a constant ^{15}N amplitude used for cross-polarization. As seen from the spectra, a linear ramp of 41.7 $\pm$ 5.6 kHz gave the highest signal/noise for all experiments. These data show that a linear ramp improves the signal/noise and emphasizes the importance of optimizing cross-polarization

2. *Optimize the CP condition for protein*. In order to find optimal matching conditions for CP, it is recommended to have a uniformly ^{15}N-labeled sample that gives at least 10:1 signal-to-noise in ~256–512 scans. Similar to that described for the single crystal, the CP values can be optimized directly on the sample by adjusting the ^{1}H power level (Fig. 4) (*see* **Note 11**).
3. *Optimize the length of the CP contact time*. In addition to the power levels, the contact time of the CP should be iteratively adjusted to maximize signal-to-noise. EmrE in aligned bicelles shows an optimal value of ~0.75 ms.
4. *^{1}H offset*. The ^{1}H offset must be set correctly in order to reduce the zero-frequency peaks. For transmembrane helical proteins in flipped bicelles, a ^{1}H offset in the range of 4.7–7 ppm will minimize the zero-frequency signals [37].
5. *Find optimal recycle delay*. The recycle delay should be set to 3–5 times the ^{1}H T_1, which can be measured using an inversion recovery experiment on the protein. For EmrE, we normally use a delay of 3 or 4 s.
6. *Acquisition of the PISEMA experiment*. Using the calibrated ^{15}N pulse powers from the single crystal and the ^{1}H pulse power from the protein sample, one can calculate the applied frequency for ^{1}H during FSLG or PMLG to match the desired effective frequency. Since the maximum ^{1}H-^{15} N dipolar couplings are ~10 kHz, we typically employ a t_1 dwell time of 48 μs for protein samples in flipped bicelles, which corresponds to an effective frequency $\omega_{\text{eff}}/2\pi = 41.7$ kHz. This spectral width is sufficient to cover the entire breadth of dipolar couplings in the indirect dimension. An example PISEMA spectrum for selectively labeled EmrE with ^{15}N methionine is shown in Fig. 5.

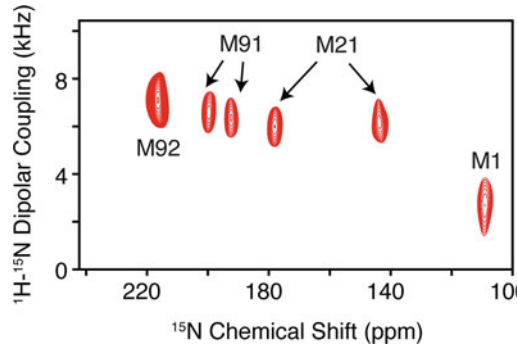

Fig. 5 PISEMA of ^{15}N methionine-labeled EmrE in DMPC/DHPC aligned bicelles. Note that M21 and M91 show clear doubling in the spectrum indicative of an asymmetric dimer. (Reproduced with permission from Ref. 27. © WILEY-VCH Verlag GmbH & Co. KgaA, Weinheim, 2013)

7. *Assignment of PISEMA spectra*. The acquired spectrum needs to be assigned in order to obtain site-resolved structural information. There are several viable approaches including the usage of site-directed mutagenesis [27], selectively labeled samples in combination with periodic wheel approximations [7, 9, 42, 43], and spectroscopic methods that make use of magnetization transfers [44, 45]. Once the assignments are obtained, these can be used as restraints in structural refinement calculations.

We have successfully employed PISEMA to show that both monomers in the functional EmrE dimer give a separate set of peaks (*see* Fig. 5). These results validated the asymmetric dimer structural models available from X-ray crystallography and cryoelectron microscopy [27, 46, 47]. Furthermore, we recently applied the pure exchange (PUREX) method [48] to investigate the conformational dynamics of EmrE in aligned bicelles that can be applied to other membrane protein systems [28]. Notably, we discovered that the change in protonation state of a conserved glutamate residue alters the conformational exchange rate of EmrE that plays a direct role in drug efflux [49].

4 Notes

1. The ability of a sample to align is very dependent on the molar ratio of DMPC:DHPC ("*q*-value"). If the q-value is significantly below 3.2 the bicelle will be isotropic.
2. The final volume of the sample should be 125 μL to ensure that the total lipid concentration is at least 25% (w/v). If the lipid concentration is too low the bicelles will not align.

3. The sample will readily align at 37 °C with the bilayer normal perpendicular with respect to the direction of the magnetic field (i.e., unflipped bicelles). Some proteins that undergo rapid uniaxial rotational diffusion can be characterized under these conditions [50]. However, our experiments show that EmrE's rotational diffusion is not sufficiently rapid to average out the residual anisotropy [51]. For this reason, the bicelle normal is "flipped" by 90° using $YbCl_3$, which orients the bilayer normal parallel to the magnetic field. These paramagnetic ions bind to the phosphate within the lipid headgroup and change the magnetic susceptibility of the bicelle [19, 21].
4. It is important to note that these spectra do not guarantee that the protein will be properly aligned in the magnetic field. However, when the bicelle containing protein is unaligned or partially aligned, our experience is that the protein's ^{15}N spectrum will give a powder pattern or be of low quality.
5. The solid-state NMR probe for PISEMA spectroscopy needs to include a sensitive detection coil optimized for ^{15}N detection. The probe designed by Gor'kov et al. [29] is the most sensitive available and uses a loop-gap resonator for the ^{1}H channel that minimizes sample heating and uses a ^{15}N solenoid for detection. The inner solenoid coil is positioned closest to the sample in order to maximize the filling factor and sensitivity for ^{15}N detection.
6. It is important to acquire a full nutation curve when first optimizing power levels to ensure accurate measurement of the 360° pulse.
7. The optimal match condition for the single crystal is typically not the best for the protein sample; however, it should be optimized to ensure sufficient signal-to-noise for calibration of the ^{15}N pulse and PISEMA experiment. The contact time can also be adjusted iteratively, but typically ~2 ms will give the highest signal-to-noise.
8. Note that the applied nutation frequency can be calculated by $\omega_1/2\pi = 250/t_{90}$, where t_{90} is equal to the length of the 90° pulse in μsec and $\omega_1/2\pi$ is given in kHz. For example, a 6 μs pulse corresponds to a frequency of 41.7 kHz.
9. We commonly employ an effective ^{1}H frequency of $\omega_{eff}/2\pi = 41.7$ kHz, an offset $\Delta\omega/2\pi = 24.1$ kHz, and an applied frequency of $\omega_1/2\pi = 34.0$ kHz. Unlike most multidimensional NMR experiments, the dwell time during the t_1 evolution period cannot be set independently from the FSLG or PMLG parameters. Specifically, the minimum t_1 dwell time is the application of two 360° pulses. This works out to give a minimum dwell time equal to $8 \times (250/(\omega_{eff}/2\pi))$. For example, with an effective frequency of $\omega_{eff}/2\pi = 41.7$ kHz, the dwell time is 48 μs.

10. The indirect ^{1}H-^{15}N dipolar coupling is scaled due to the Lee-Goldburg sequence and needs to be adjusted by the scaling factor (0.82) to give the correct couplings [26]. For example, a dwell time of 48 μs during FSLG or PMLG gives a corrected spectral width of 25.4 kHz.
11. For selectively labeled samples, the signal-to-noise often prevents detailed optimization of pulse parameters. However, since the buffer composition is the same as that of the uniformly ^{15}N-labeled sample, the optimal values typically do not vary significantly.

Acknowledgments

This work was supported by NIH (R01AI108889) and NSF (MCB1506420). M.L. acknowledges support from a Margaret-Strauss Kramer Fellowship.

References

1. Nikaido H (2009) Multidrug resistance in bacteria. Annu Rev Biochem 78:119–146. https://doi.org/10.1146/annurev.biochem.78.082907.145923
2. Nikaido H, Pages JM (2012) Broad-specificity efflux pumps and their role in multidrug resistance of Gram-negative bacteria. FEMS Microbiol Rev 36(2):340–363. https://doi.org/10.1111/j.1574-6976.2011.00290.x
3. Allen HK, Donato J, Wang HH, Cloud-Hansen KA, Davies J, Handelsman J (2010) Call of the wild: antibiotic resistance genes in natural environments. Nat Rev Microbiol 4:251–259
4. Du D, van Veen HW, Murakami S et al (2015) Structure, mechanism and cooperation of bacterial multidrug transporters. Curr Opin Struct Biol 33:76–91. https://doi.org/10.1016/j.sbi.2015.07.015
5. Traaseth NJ, Shi L, Verardi R et al (2009) Structure and topology of monomeric phospholamban in lipid membranes determined by a hybrid solution and solid-state NMR approach. Proc Natl Acad Sci U S A 106 (25):10165–10170. https://doi.org/10.1073/pnas.0904290106
6. Vostrikov Vitaly V, Grant Christopher V, Opella Stanley J et al (2011) On the combined analysis of (2)H and (15)N/(1)H solid-state NMR data for determination of transmembrane peptide orientation and dynamics. Biophys J 101(12):2939–2947. https://doi.org/10.1016/j.bpj.2011.11.008
7. Marassi FM, Opella SJ (2000) A solid-state NMR index of helical membrane protein structure and topology. J Magn Reson 144 (1):150–155. https://doi.org/10.1006/jmre.2000.2035
8. Cross TA (1986) A solid state nuclear magnetic resonance approach for determining the structure of gramicidin a without model fitting. Biophys J 49(1):124–126
9. Wang J, Denny J, Tian C et al (2000) Imaging membrane protein helical wheels. J Magn Reson 144(1):162–167. https://doi.org/10.1006/jmre.2000.2037
10. Buffy JJ, Traaseth NJ, Mascioni A et al (2006) Two-dimensional solid-state NMR reveals two topologies of sarcolipin in oriented lipid bilayers. Biochemistry 45(36):10939–10946. https://doi.org/10.1021/bi060728d
11. Opella SJ, Marassi FM (2004) Structure determination of membrane proteins by NMR spectroscopy. Chem Rev 104(8):3587–3606. https://doi.org/10.1021/cr0304121
12. Clark NA, Rothschild KJ, Luippold DA et al (1980) Surface-induced lamellar orientation of multilayer membrane arrays. Theoretical analysis and a new method with application to purple membrane fragments. Biophys J 31 (1):65–96. https://doi.org/10.1016/S0006-3495(80)85041-7
13. Moll F 3rd, Cross TA (1990) Optimizing and characterizing alignment of oriented lipid bilayers containing gramicidin D. Biophys J

57(2):351–362. https://doi.org/10.1016/S0006-3495(90)82536-4

14. Sanders Ii CR, Hare BJ, Howard KP et al (1994) Magnetically-oriented phospholipid micelles as a tool for the study of membrane-associated molecules. Prog Nucl Magn Reson Spectrosc 26(Part 5):421–444. https://doi.org/10.1016/0079–6565(94)80012-X
15. Song Z, Kovacs FA, Wang J et al (2000) Transmembrane domain of M2 protein from influenza a virus studied by solid-state 15N polarization inversion spin exchange at magic angle NMR. Biophys J 79(2):767–775. https://doi.org/10.1016/S0006-3495(00)76334-X
16. Traaseth NJ, Verardi R, Torgersen KD et al (2007) Spectroscopic validation of the pentameric structure of phospholamban. Proc Natl Acad Sci U S A 104(37):14676–14681. https://doi.org/10.1073/pnas.0701016104
17. De Angelis AA, Opella SJ (2007) Bicelle samples for solid-state NMR of membrane proteins. Nat Protoc 2(10):2332–2338
18. Sanders CR, Schwonek JP (1992) Characterization of magnetically orientable bilayers in mixtures of dihexanoylphosphatidylcholine and dimyristoylphosphatidylcholine by solid-state NMR. Biochemistry 31(37):8898–8905. https://doi.org/10.1021/bi00152a029
19. Marcotte I, Auger M (2005) Bicelles as model membranes for solid- and solution-state NMR studies of membrane peptides and proteins. Concepts Magn Reson A 24A(1):17–37. https://doi.org/10.1002/cmr.a.20025
20. Warschawski DE, Arnold AA, Beaugrand M et al (2011) Choosing membrane mimetics for NMR structural studies of transmembrane proteins. Biochim Biophys Acta Biomembr 1808(8):1957–1974. https://doi.org/10.1016/j.bbamem.2011.03.016
21. Prosser RS, Hwang JS, Vold RR (1998) Magnetically aligned phospholipid bilayers with positive ordering: a new model membrane system. Biophys J 74(5):2405–2418. https://doi.org/10.1016/S0006-3495(98)77949-4
22. Yamamoto K, Pearcy P, Ramamoorthy A (2014) Bicelles exhibiting magnetic alignment for a broader range of temperatures: a solid-state NMR study. Langmuir 30(6):1622–1629. https://doi.org/10.1021/la404331t
23. Yamamoto K, Pearcy P, Lee D-K et al (2015) Temperature-resistant bicelles for structural studies by solid-state NMR spectroscopy. Langmuir 31(4):1496–1504. https://doi.org/10.1021/la5043876
24. Triba MN, Devaux PF, Warschawski DE (2006) Effects of lipid chain length and unsaturation on bicelles stability. A phosphorus NMR study. Biophys J 91(4):1357–1367. https://doi.org/10.1529/biophysj.106.085118
25. Wu C, Ramamoorthy A, Opella S (1994) High-resolution heteronuclear dipolar solid-state NMR spectroscopy. J Magn Reson 109A:270–272
26. Ramamoorthy A, Wei Y, Lee D-K (2004) PISEMA solid-state NMR spectroscopy. In: Annual reports on NMR spectroscopy, vol 52. Academic Press, London, pp 1–52. https://doi.org/10.1016/S0066-4103(04)52001-X
27. Gayen A, Banigan JR, Traaseth NJ (2013) Ligand-induced conformational changes of the multidrug resistance transporter EmrE probed by oriented solid-state NMR spectroscopy. Angew Chem Int Ed 52(39):10321–10324. https://doi.org/10.1002/anie.201303091
28. Cho M-K, Gayen A, Banigan JR et al (2014) Intrinsic conformational plasticity of native EmrE provides a pathway for multidrug resistance. J Am Chem Soc 136(22):8072–8080. https://doi.org/10.1021/ja503145x
29. Gor'kov PL, Chekmenev EY, Li C et al (2007) Using low-E resonators to reduce RF heating in biological samples for static solid-state NMR up to 900 MHz. J Magn Reson 185(1):77–93. https://doi.org/10.1016/j.jmr.2006.11.008
30. Delaglio F, Grzesiek S, Vuister GW et al (1995) NMRPipe: a multidimensional spectral processing system based on UNIX pipes. J Biomol NMR 6(3):277–293. https://doi.org/10.1007/bf00197809
31. Fung BM, Khitrin AK, Ermolaev K (2000) An improved broadband decoupling sequence for liquid crystals and solids. J Magn Reson 142(1):97–101. https://doi.org/10.1006/jmre.1999.1896
32. Bielecki ACK, De Groot HJM, Griffin RG, Levitt MH (1990) Frequency-switched Lee--Goldburg sequence in solids. Adv Magn Reson 14:111–150
33. Goldburg WG, Lee M (1965) Nuclear magnetic resonance line narrowing by a rotation RF field. Phys Rev 140:1261–1271
34. Vinogradov E, Madhu PK, Vega S (1999) High-resolution proton solid-state NMR spectroscopy by phase-modulated Lee–Goldburg experiment. Chem Phys Lett 314(5–6):443–450. https://doi.org/10.1016/S0009-2614(99)01174-4
35. Fu R, Tian C, Cross TA (2002) NMR spin locking of proton magnetization under a

frequency-switched Lee–Goldburg pulse sequence. J Magn Reson 154(1):130–135. https://doi.org/10.1006/jmre.2001.2468

36. Yamamoto K, Lee DK, Ramamoorthy A (2005) Broadband-PISEMA solid-state NMR spectroscopy. Chem Phys Lett 407 (4–6):289–293. https://doi.org/10.1016/j.cplett.2005.03.082
37. Gopinath T, Traaseth NJ, Mote K et al (2010) Sensitivity enhanced heteronuclear correlation spectroscopy in multidimensional solid-state NMR of oriented systems via chemical shift coherences. J Am Chem Soc 132 (15):5357–5363. https://doi.org/10.1021/ja905991s
38. Veglia TGaG (2009) Sensitivity enhancement in static solid-state NMR experiments via single- and multiple-quantum dipolar coherences. J Am Chem Soc 131(16):5754–5756
39. Gopinath T, Veglia G (2010) Improved resolution in dipolar NMR spectra using constant time evolution PISEMA experiment. Chem Phys Lett 494(1–3):104–110. https://doi.org/10.1016/j.cplett.2010.05.078
40. Koroloff SN, Nevzorov AA (2015) Optimization of cross-polarization at low radiofrequency fields for sensitivity enhancement in solid-state NMR of membrane proteins reconstituted in magnetically aligned bicelles. J Magn Reson 256:14–22. https://doi.org/10.1016/j.jmr.2015.03.016
41. Tang W, Nevzorov AA (2011) Repetitive cross-polarization contacts via equilibration-re-equilibration of the proton bath: sensitivity enhancement for NMR of membrane proteins reconstituted in magnetically aligned bicelles. J Magn Reson 212(1):245–248. https://doi.org/10.1016/j.jmr.2011.06.028
42. Bertram R, Quine JR, Chapman MS et al (2000) Atomic refinement using orientational restraints from solid-state NMR. J Magn Reson 147(1):9–16. https://doi.org/10.1006/jmre.2000.2193
43. De Angelis AA, Howell SC, Nevzorov AA et al (2006) Structure determination of a membrane protein with two trans-membrane helices in aligned phospholipid bicelles by solid-state NMR spectroscopy. J Am Chem Soc 128 (37):12256–12267. https://doi.org/10.1021/ja063640w
44. Traaseth NJ, Gopinath T, Veglia G (2010) On the performance of spin diffusion NMR techniques in oriented solids: prospects for resonance assignments and distance measurements from separated local field experiments. J Phys Chem B 114(43):13872–13880. https://doi.org/10.1021/jp105718r
45. Nevzorov AA (2008) Mismatched Hartmann−Hahn conditions cause proton-mediated intermolecular magnetization transfer between dilute low-spin nuclei in NMR of static solids. J Am Chem Soc 130 (34):11282–11283. https://doi.org/10.1021/ja804326b
46. Fleishman SJ, Harrington SE, Enosh A et al (2006) Quasi-symmetry in the cryo-EM structure of EmrE provides the key to modeling its transmembrane domain. J Mol Biol 364 (1):54–67. https://doi.org/10.1016/j.jmb.2006.08.072
47. Chen Y-J, Pornillos O, Lieu S et al (2007) X-ray structure of EmrE supports dual topology model. Proc Natl Acad Sci U S A 104 (48):18999–19004. https://doi.org/10.1073/pnas.0709387104
48. deAzevedo ER, Bonagamba TJ, Schmidt-Rohr K (2000) Pure-exchange solid-state NMR. J Magn Reson 142(1):86–96. https://doi.org/10.1006/jmre.1999.1918
49. Gayen A, Leninger M, Traaseth NJ (2016) Protonation of a glutamate residue modulates the dynamics of the drug transporter EmrE. Nat Chem Biol 12(3):141–145. https://doi.org/10.1038/nchembio.1999. http://www.nature.com/nchembio/journal/v12/n3/abs/nchembio.1999.html—supplementary-information
50. Lu GJ, Opella SJ (2014) Resonance assignments of a membrane protein in phospholipid bilayers by combining multiple strategies of oriented sample solid-state NMR. J Biomol NMR 58(1):69–81. https://doi.org/10.1007/s10858-013-9806-y
51. Banigan JR, Gayen A, Traaseth NJ (2015) Correlating lipid bilayer fluidity with sensitivity and resolution of polytopic membrane protein spectra by solid-state NMR spectroscopy. Biochim Biophys Acta 1848(1, Part B):334–341. https://doi.org/10.1016/j.bbamem.2014.05.003